(Delacourte et al., 1999). The data support the notion that functional abnormality in the parietal association areas should be a *better predictor* of AD conversion. However, two longitudinal studies (Huang et al., 2002; Drzezga et al., 2003) suggested high predictive value of functional abnormality in the PCC; further study will be needed to clarify the predictive value of the functional abnormality in the PCC.

Unexpectedly, we found decreased rCBF in the right caudate nucleus in comparing controls and non-converters. A recent voxel-based volumetric MR study (Frisoni et al., 2002) revealed reduced gray matter volume of caudate nucleus in mild AD; however, we have no good explanation or hypothesis about this finding at the present moment.

Reduction of rCBF in the parahippocampal gyrus in converters

In this study, we found reduced parahippocampal rCBF in converters. Numerous structural MRI studies have demonstrated that progressive atrophy of the parahippocampal area including the entorhinal cortex is a sensitive marker for detecting and predicting AD (Chetelat and Baron, 2003; Korf et al., 2004; Nestor et al., 2004). In this study, we did not apply a partial volume effect (PVE) correction for SPECT imaging; therefore, one could argue that reduced rCBF in the parahippocampal area could be explained by partial volume effect. We agree that PVE partially contributes to the results of our study. However, an atrophy-corrected FDG-PET study demonstrated hippocampal hypometabolism in AD and MCI and the study's authors concluded that metabolism reductions exceed volume losses in MCI (De Santi et al., 2001). Other studies with MRI-guided FDG-PET also demonstrated hypometabolism of the limbic systems (de Leon et al., 2001; Nestor et al., 2003a,b) including the entorhinal cortex in MCI.

Limitations of this study

The first limitation of this study is that we did not evaluate the cross-validity of the predictive value of the SPECT findings using split-half reliability due to the limited number of non-converters. To conclude the usefulness of rCBF SPECT in predicting AD conversion, our data should be replicated in other cohorts. In this context, our data may be considered to be preliminary rather than conclusive. However, other studies conducted by different research groups using a different imaging method (FDG-PET) reported similar results to those of the present study (Chetelat et al., 2003), and we believe that our predictive model should be reliable.

Second, we did not perform the correction of partial volume effects (PVE) for SPECT images. We agree that PVE could partially contribute to the results of the present study. Even so, the predictive value of rCBF patterns identified in this study still has diagnostic value. From a diagnostic point of view, atrophy-related hypoperfusion is a consequence of AD pathology and might improve the detection of early functional abnormalities.

Finally, some may argue that a 3-year follow-up is not long enough. We agree that it remains a possibility that some of the non-converters would develop AD during a longer observation period, because the logistic model cannot be certain that someone will not convert AD after the follow-up period. However, we can still distinguish rapid converters from slow converters or slow decliners using the initial SPECT study. The results suggest that the initial SPECT study can discriminate between rapid decliners and slow decliners. Such discrimination is important for both therapeutic and research purposes.

Conclusion

We demonstrated that the rCBF reductions in the parietal association areas and the precunei are a good predictor of progression from MCI to AD. The data suggest that the initial rCBF SPECT in individuals with MCI could be a promising method to accurately predict who would meet diagnostic criteria for AD in the next 3 years.

Acknowledgment

This study was supported by the Promotion of Fundamental Studies in Health Science of Organization for Pharmaceuticals and Medical Devices Agency.

References

American Psychiatric Association, 1994. Diagnostic and Statistical Manual of Mental Disorders. DSM-IV (4th ed.). American Psychiatric Association, Washington, DC.

Arnaiz, E., Jelic, V., Almkvist, O., Wahlund, L.O., Winblad, B., Valind, S., et al., 2001. Impaired cerebral glucose metabolism and cognitive functioning predict deterioration in mild cognitive impairment. NeuroReport 12, 851–855.

Bruscoli, M., Lovestone, S., 2004. Is MCI really just early dementia? A systematic review of conversion studies. Int. Psychogeriatr. 16, 129–140.

Celsis, P., Agniel, A., Cardebat, D., Demonet, J.F., Ousset, P.J., Puel, M., 1997. Age related cognitive decline: a clinical entity? A longitudinal study of cerebral blood flow and memory performance. J. Neurol. Neurosurg. Psychiatry 62, 601–608.

Chetelat, G., Baron, J.C., 2003. Early diagnosis of Alzheimer's disease: contribution of structural neuroimaging. NeuroImage 18, 525–541.

Chetelat, G., Desgranges, B., de la Sayette, V., Viader, F., Eustache, F., Baron, J.C., 2003. Mild cognitive impairment: can FDG-PET predict who is to rapidly convert to Alzheimer's disease? Neurology 60, 1374–1377.

de Leon, M.J., Convit, A., Wolf, O.T., Tarshish, C.Y., DeSanti, S., Rusinek, H., et al., 2001. Prediction of cognitive decline in normal elderly subjects with 2-[(18)F]fluoro-2-deoxy-D-glucose/poitron-emission tomography (FDG/PET). Proc. Natl. Acad. Sci. U. S. A. 98, 10966–10971.

De Santi, S., de Leon, M.J., Rusinek, H., Convit, A., Tarshish, C.Y., Roche, A., et al., 2001. Hippocampal formation glucose metabolism and volume losses in MCI and AD. Neurobiol. Aging 22, 529–539.

Delacourte, A., David, J.P., Sergeant, N., Buee, L., Wattez, A., Vermersch, P., et al., 1999. The biochemical pathway of neurofibrillary degeneration in aging and Alzheimer's disease. Neurology 52, 1158–1165.

Drzezga, A., Lautenschlager, N., Siebner, H., Riemenschneider, M., Willoch, F., Minoshima, S., et al., 2003. Cerebral metabolic changes accompanying conversion of mild cognitive impairment into Alzheimer's disease: a PET follow-up study. Eur. J. Nucl. Med. Mol. Imaging 30, 1104–1113.

Folstein, M.F., Folstein, S.E., McHugh, P.R., 1975. "Mini-mental state". A practical method for grading the cognitive state of patients for the clinician. J. Psychiatr. Res. 12, 189–198.

Frisoni, G.B., Testa, C., Zorzan, A., Sabattoli, F., Beltramello, A., Soininen, H., et al., 2002. Detection of grey matter loss in mild Alzheimer's disease with voxel based morphometry. J. Neurol. Neurosurg. Psychiatry. 73, 657–664.

Hamilton, M., 1960. A rating scale for depression. J. Neurol. Neurosurg. Psychiatry 23, 56–62.

Huang, C., Wahlund, L.O., Svensson, L., Winblad, B., Julin, P., 2002. Cingulate cortex hypoperfusion predicts Alzheimer's disease in mild cognitive impairment. BMC Neurol. 2, 9.

Hughes, C.P., Berg, L., Danziger, W.L., Coben, L.A., Martin, R.L., 1982. A new clinical scale for the staging of dementia. Br. J. Psychiatry 140, 566–572.

Imabayashi, E., Matsuda, H., Asada, T., Ohnishi, T., Sakamoto, S., Nakano, S., et al., 2004. Superiority of 3-dimensional stereotactic surface projection analysis over visual inspection in discrimination of patients with very early Alzheimer's disease from controls using brain perfusion SPECT. J. Nucl. Med. 45, 1450–1457.

Jack Jr., C.R., Petersen, R.C., Xu, Y.C., O'Brien, P.C., Smith, G.E., Ivnik, R.J., 1999. Prediction of AD with MRI-based hippocampal volume in mild cognitive impairment. Neurology 52, 1397–1403.

Kogure, D., Matsuda, H., Ohnishi, T., Asada, T., Uno, M., Kunihiro, T., et al., 2000. Longitudinal evaluation of early Alzheimer's disease using brain perfusion SPECT. J. Nucl. Med. 41, 1155–1162.

Korf, E.S., Wahlund, L.O., Visser, P.J., Scheltens, P., 2004. Medial temporal lobe atrophy on MRI predicts dementia in patients with mild cognitive impairment. Neurology 63, 94–100.

McKhann, G., Drachman, D., Folstein, M., Katzman, R., Price, D., Stadlan, E.M., 1984. Clinical diagnosis of Alzheimer's disease: report of the NINCDS-ADRDA Work Group under the auspices of Department of Health and Human Services Task Force on Alzheimer's Disease. Neurology 34, 939–944.

Minoshima, S., Giordani, B., Berent, S., Frey, K.A., Foster, N.L., Kuhl, D.E., 1997. Metabolic reduction in the posterior cingulate cortex in very early Alzheimer's disease. Ann. Neurol. 42, 85–94.

Mosconi, L., Perani, D., Sorbi, S., Herholz, K., Nacmias, B., Holthoff, V., Salmon, E., Baron, J.C., De Cristofaro, M.T., Padovani, A., Borroni, B., Franceschi, M., Bracco, L., Pupi, A., 2004. MCI conversion to dementia and the APOE genotype: a prediction study with FDG-PET. Neurology 63, 2332–2340.

Mungas, D., Reed, B.R., Jagust, W.J., DeCarli, C., Mack, W.J., Kramer, J.H., et al., 2002. Volumetric MRI predicts rate of cognitive decline related to AD and cerebrovascular disease. Neurology 59, 867–873.

Nestor, P.J., Fryer, T.D., Ikeda, M., Hodges, J.R., 2003a. Retrosplenial cortex (BA 29/30) hypometabolism in mild cognitive impairment (prodromal Alzheimer's disease). Eur. J. Neurosci. 18, 2663–2667.

Nestor, P.J., Fryer, T.D., Smielewski, P., Hodges, J.R., 2003b. Limbic hypometabolism in Alzheimer's disease and mild cognitive impairment. Ann. Neurol. 54, 343–351.

Nestor, P.J., Scheltens, P., Hodges, J.R., 2004. Advances in the early detection of Alzheimer's disease. Nat. Med. 10, S34–S41 (Suppl.).

Palmer, K., Fratiglioni, L., Winblad, B., 2003. What is mild cognitive impairment? Variations in definitions and evolution of nondemented persons with cognitive impairment. Acta Neurol. Scand., Suppl. 179, 14–20.

Petersen, R.C., Doody, R., Kurz, A., Mohs, R.C., Morris, J.C., Rabins, P.V., et al., 2001a. Current concepts in mild cognitive impairment. Arch. Neurol. 58, 1985–1992.

Petersen, R.C., Stevens, J.C., Ganguli, M., Tangalos, E.G., Cummings, J.L., DeKosky, S.T., 2001b. Practice parameter: early detection of dementia: mild cognitive impairment (an evidence-based review). Report of the Quality Standards Subcommittee of the American Academy of Neurology. Neurology 56, 1133–1142.

Reiman, E.M., Chen, K., Alexander, G.E., Caselli, R.J., Bandy, D., Osborne, D., et al., 2004. Functional brain abnormalities in young adults at genetic risk for late-onset Alzheimer's dementia. Proc. Natl. Acad. Sci. U. S. A. 101, 284–289.

Talairach, J., Tournoux, P., 1988. Co-planar Stereotaxic Atlas of the Human Brain. Thieme, Stuttgart.

Journal of Deaf Studies and Deaf Education Advance Access published November 30, 2005

Neural Correlates for Numerical Processing in the Manual Mode

Nobuo Masataka
Kyoto University
The Japan Science and Technology Agency
Takashi Ohnishi
Etsuko Imabayashi
Makiko Hirakata
Hiroshi Matsuda
National Center for Neurology and Psychiatry

This paper reports a study designed to examine the neuronal correlates for comprehending the signs of American Sign Language representing numerals in deaf signers who acquired Japanese Sign Language as their first language. The participants were scanned by functional magnetic resonance imaging (fMRI) twice on the day of the experiment. The results of the measurements revealed that upon learning that the signs actually have numeric meaning, a network of brain areas is activated immediately. Many of these areas have been previously implicated in numerical processing. The similar neural network of brain regions responsible for numerical processing exists on a nonlinguistical basis and works to retrieve arithmetic facts from presented linguistic material regardless of the mode of the language.

Digits and number words are considered a very recent cultural invention in the evolution of the human species. Indeed, they arise from the specifically human and evolutionarily recent ability to create and mentally manipulate complex symbols. The sense of numerosity, however, is older. Many animals are sensitive to numerical regularities in their environments, can represent these regularities internally, and can perform elementary and approximate computations with numerical quantities (Gallistel, 1990; McComb, Packer, & Pusey, 1994; Suzuki & Kobayashi, 2000). Similar abilities are found in human infants in their first year of life, well before they begin to produce language (e.g., Xu & Spelke, 2000). These converging lines of evidence suggest the existence in the animal and human brain of specialized neural systems for processing numbers on a nonlinguistical basis (Kobayashi, Hiraki, Mugitani, & Hasegawa, 2004).

Substantial experimental evidence points to the notion that such domain-specific mechanism, or a core "number sense," accounts for our uniquely human talent for formal mathematics. Several lines of evidence from studies of numerical competence in normal adults, infants, and young children, who are all hearing, as well as in nonhuman animals has led many researchers to conclude that the domain-specific system of knowledge, present in many species, is responsible for the sense of number and forms the basis for the complex symbolic manipulation of number developed by humans (Dehaene, 1997; Gallistel & Gelman, 1992).

Particularly, the findings reported by Barth, Kanwisher, and Spelke (2003), Dehaene, Dupoux, and Mehler (1990), and Xu and Spelke (2000) should be noticeable, in which many tasks that deal explicitly with exact symbolic numerosities automatically activate nonsymbolic number representations. More recently, Barth et al. (in press) investigated this issue more directly in examining whether hearing adults and hearing preschool children can perform simple arithmetic calculations on nonsymbolic numerosities. Results of the five experiments they conducted clearly

This work was partly supported by a Health Science Research Grant from the Ministry of Health, Labor and Welfare (H13-005), Center of Research for Excellent Study and Technology (CREST), Japan Science and Technology Agency, and 21st Century Grant-in-Aid Research for Center of Excellence (COE), Kyoto University. Open Access charges for this paper were provided by CREST and the 21st Grant for the COE. Correspondence should be sent to Nobuo Masataka, Primate Research Institute, Kyoto University, Inuyama, Aichi 484-8506, Japan (e-mail: masataka@pri.kyoto-u.ac.jp).

 doi:10.1093/deafed/enj017

reveal that both the adults and the children with no training in arithmetic successfully performed approximate arithmetic on large sets of elements. Success at these tasks did not depend on nonnumerical continuous quantities, modality-specific quantity information, or the adoption of alternative nonarithmetic knowledge. Thus, they concluded that abstract numerical quantity representations are computationally functioned and may provide a foundation for formal mathematics.

Such reasoning is also quite consistent with a recent neuronal model for the implementation of elementary numerical abilities proposed based on the findings from a series of brain-imaging experiments (see Piazza & Dehaene, 2005, for a review). Piazza and Dehaene (2005) claim that mathematical ability results from the integration of two nonnumerical neural circuits in the brain: the left frontal lobe, which controls linguistic representations of exact numerical values, and the parietal lobes, which control visuospatial representations of approximate quantities. According to their view, humans have at least two means of representing and processing quantity. One is the ability to make perceptually based judgments and comparisons, in which the degree of accuracy varies with set size. The other allows precise quantification through the use of symbols, concepts, and rules. Arithmetical tasks that require exact numerical answers depend on verbal representations of numbers, whereas tasks requiring estimation or approximation depend on nonlinguistic representations of approximate quantities.

In all, it appears that a region of parietal cortex underlies an abstract-semantic number sense and a region of left prefrontal cortex underlies more specific operations mediating exact or approximate calculation. The notion is compelling and provocative. Indeed, there is a growing literature that presents neuronal evidence for the explanation given by Dehaene and his colleagues (see Piazza & Dehaene, 2005, for review). However, it should be noted that all such previous studies about numerical processing, whether cognitive ones or neurological ones, have pursued this issue in hearing subjects who had acquired a spoken language as their first language by presenting digits or number words in written form. None of these studies have worked with deaf subjects who had acquired a signed language as their first language though naturally evolved signed languages, even though such subjects are known to possess identical levels of linguistic organization, including phonology, morphology, syntax, and semantics (Klima & Bellugi, 1979; Padden, 1988). In fact, recent investigations into languages have provided a powerful research opportunity for exploring the neural basis of the human brain that works in conjunction in both the manual and vocal modes for the purpose of language organization (Emmorey, 2002; Masataka, 2003).

Having extended such reasoning into the research field of numerical processing, recently, Masataka (in press) investigated the capacity for nonsymbolic arithmetic performance in deaf adults who acquired Japanese Sign Language (JSL) as their first language as well as in hearing adults. In the study, the participants performed the numerical subtraction task on large sets of elements, presented as visual arrays of dots, for the testing of the capacity for nonsymbolic arithmetic performance. For the task, the participants were presented with three visual arrays of dots and were asked to subtract the second array from the first and to compare this difference to the number of elements in the third array (e.g., "56 − 16 = (40) vs. 35). The results revealed that they could perform simple arithmetic subtraction on nonsymbolic numerosities. Their performance levels were even higher than those of hearing adults who participated in the experiment as a control group.

Based on these findings, therefore, we attempted to conduct neuropsychological research as a next step. Namely, we hypothesized that the neural network of brain areas for numerical processing would also exist on a nonlinguistical basis in the deaf adults who participated in the experiment of Masataka (in press) and that it should function normally for the retrieving of arithmetic facts from presented stimuli independent of any modality difference in the language by which the presented stimuli are coded. In order to test this here, we have undertaken the present experiment with the participants by presenting signs of American Sign Language (ASL) representing numerals. Before the experiment, participants were totally naive to ASL. During the experiment we compared brain activation in the participants both before and after learning the coded representations in the presented ASL signs with

the use of functional magnetic resonance imaging (fMRI). Once these representations are learned, a change in brain activation is thought to accompany the transcoding of the numerals. We hypothesized that the network should extensively share the brain regions that have been previously been implicated in the numerical processing studies by Dehaene and his colleagues (Dehaene, 1997; Dehaene et al., 1999).

Method

Participants

Participants were 13 right-handed profoundly deaf adults (8 males and 5 females) varying in age between 19 and 50, and their parents were all hearing. They were all involved in the study by Masataka (in press). Though they had acquired JSL as their first language, the deaf participants were first exposed to JSL at the age of 3 years when they were first diagnosed to be profoundly deaf. Thereafter, they started to attend the educational program by JSL every weekday with their parents. Until then, their parents were not knowledgeable about any form of signed language. The participants learned Japanese in written form through an official elementary education, which started when they were 6–7 years old. All the participants in the group of hearing adults had normal hearing. They spoke Japanese as their first language and had never been exposed to any form of signed language before. Before this study, the participants were totally naive to ASL or Finger Alphabet.

Overall Design

Neuroimaging experiments are becoming easier to carry out with the increasing availability of fMRI scanners. Preprocessing steps are being streamlined and automated, enabling data to be processed faster and more easily. Using fMRI to visualize function in vivo, neuroscientists have demonstrated that the mental operations conducted by the human brain can be empirically measured. Typically, epoch or block experimental designs have been the workhorse of such experimentation. In these designs, stimuli are presented for a period of seconds and alternated randomly or pseudorandomly over the course of the data acquisition period. Usually two different groups of stimuli are prepared: one as task stimuli and the other as control stimuli. The blood-oxygen-level-dependent (BOLD) signals are to be compared between the two stimulus conditions so that we could evaluate the effects of some characteristics provided with the task stimuli, which are not present in the control stimuli. So far, we have undertaken several neuroimaging studies with this experimental paradigm (Masataka, Ohnishi, Imabayashi, Hirakata, & Matsuda, 2005; Ohnishi et al., 2001, 2004), and the present experiment was also undertaken with the same design.

In the present experiment, testing with fMRI was undertaken twice in a single day with the presentation of the same set of stimuli to the same group of participants. In each testing, strings of four to six ASL signs, each of which represented a number between 1,000 and 4,000, were presented on a monitor as task stimuli. For control stimuli, a sign was randomly chosen from the repertoire of the Finger Alphabet described by Shioda (1985) as a counterpart to each ASL sign used, and strings of such signs were presented. The finger movements were close to those of spelling with the index finger of some capital letters of the alphabet, such as X and Q.

The participants' cerebral activation in response to the ASL signs was measured by subtracting the activation level of BOLD signals recorded when the control stimuli were presented from that recorded when the task stimuli were presented in each testing. After the first testing, the participants were instructed about the meaning of each of the ASL signs used in the experiment. However, they remained naive to Finger Alphabet. Thereafter, they received the second testing. Whereas, in the first testing, not only the control stimuli but also the task stimuli were perceived as meaningless by the participants, the task stimuli became meaningful in the second testing. By comparing the cerebral activation between the first and the second testing, we attempted to examine its practice-related changes if any.

Procedure

Each of the participants received their first testing with fMRI measurement, in which they were instructed to simply "Recognize the meaning of the presented

stimulus, which has been chosen from a foreign signed language system." When this testing was finished, the participants' performance with regard to comprehension of the stimuli was scored without the fMRI measurement. In the scoring of performance, each participant was presented with the same set of combinations of signs as those used in the testing with the fMRI measurement. The participants were instructed to write an Arabic number represented by each combination of signs consecutively presented on the monitor of a personal computer at 3-s intervals. Thereafter, the participants were taught about the meaning of each ASL sign used in the testing. They received "exercises" to decode the meaning by producing a JSL sign of the same meaning. In a given such practice trial, a give single ASL sign was presented, and the practice continued until the participants made "correct answers" in 10 consecutive trials. Actually it took approximately 20 min on the average. Upon completion of the exercises, testing with the fMRI measurement was conducted again (second testing). As soon as the second testing was finished, their performance with regard to comprehension of the stimuli was scored again without the fMRI measurement according to the same protocol as that used after the first testing.

fMRI Analysis

Measurement of cerebral activation was conducted using BOLD contrast with a 1.5 T MAGNETOM Vision plus MR scanner (Siemens, Erlangen, Germany) using a standard head coil. After automatic shimming, a time course series of 110 volumes was obtained using single-shot gradient-refocused echo-planar imaging (TR = 4,000 ms, TE = 60 s, flip angle = 90 degrees, in-plane resolution = 3.44 × 3.44 mm, FOV = 22 cm, and contiguous 4-mm slices to cover the entire brain). Head motion was minimized by placing tight but comfortable foam padding around the participant's head. The fMRI protocol was a block design with epochs in which either the task stimuli or the control stimuli were presented. Each epoch lasted 20 s (equivalent to five whole-brain fMRI volume acquisitions). The stimuli were presented using Presentation (neurobehavioral systems) running on a PC and back-projected onto a screen located approximately 50 cm from the subject's head using a 65536-color liquid crystal display and an overhead projector. Participants viewed the screen through a mirror attached to the head coil. The first five volumes of each fMRI scan were discarded because of the nonsteady condition of the magnetization, and the remaining 70 volumes were used for analysis.

Data were analyzed with Statistical Parametric mapping software (SPM99, 1999). Scans were realigned and spatially normalized to the standard stereotactic space of Talairach using an EPI template (Talairach & Tournoux, 1988). The parameter for affine and quadratic transformation to the EPI template that was already fitted to Talairach space was estimated by least squares means. Data were then smoothed in a spatial domain (full width at half maximum = 8 × 8 × 8 mm) to improve the signal-to-noise ratio. After specifying the appropriate design matrix with a delayed box-car function as a reference waveform, condition, slow homodynamic fluctuation (unrelated to the task), and subject effects were estimated according to the general linear model and taking temporal smoothness into account. Global normalization was performed using proportional scaling. To test the hypotheses about regionally specific condition effects, the estimates were compared by means of linear contrasts between each control and task period. The resulting set of voxel values for each contrast constituted a statistical parametric map of the t statistic SPM $\{t\}$. To account for interindividual variance, all group analyses were computed using a random-effects model. Further, group analyses across participants involved a one-sample t test on the images generated by pooling over the session of individual contrasts of activation versus control for each participant. In order to evaluate the learning of ASL signs, effects at the first and second testing were analyzed by a paired t test. For these group analyses, we set $p < .001$ without a correction for multiple comparisons in order to avoid Type II error, and this was followed by applying small volume correction ($p < .01$) to each cluster to avoid Type I error. The resulting sets of t values constituted the statistical parametric maps {SPM (t)}. Anatomic localization was identified using both MNI coordinates and Talairach coordinates obtained from M. Brett's transformations

(Brett, Johnsrude, & Owen, 2002) and were presented as Talairach coordinates (Talairach & Tournoux, 1988).

Results

In the first testing, clusters of activated voxels were identified only in the left visual association areas (Table 1 and Figure 1). Once the participants had been instructed on how to comprehend presented ASL signs, however, the areas of activation became widespread dramatically. The regions included the bilateral prefrontal cortex, the left premotor area, the bilateral parietal lobules, and the left middle temporal gyrus as well as the visual association areas.

The areas of the brain where significant increases in BOLD activation levels from the first to second testing were observed included the left prefrontal cortex, the bilateral parietal lobules, and the left middle temporal gyrus (Table 2 and Figure 2), but no decrease was found in any brain region. Results of the scoring with regard to performance on both the ASL number and Finger Alphabet tasks, which were conducted after the first and second fMRI measurements, revealed that the percentage of correct responses was 0% for all participants in both scoring sessions and that no participant could answer correctly in response to any stimulus. So, activation changed to what were now seen as linguistic stimuli, even though participants could not respond correctly to them.

Discussion

Even at the onset of the experiment, the ASL signs were perceived differently from the signs of the Finger Alphabet, and the activation of the visual association area was greater in response to the ASL signs than to the signs of the Finger Alphabet. This might be mostly due to the fact that ASL is a naturally evolving signed language system, whereas the Finger Alphabet used here was developed for the subsidiary means of promoting the oral education of deaf children (Shioda, 1985). Given the fact that the participants had been exposed to JSL after birth, they could have exhibited a perceptual preference for the ASL stimuli over the signs of the Finger Alphabet due to their previous experience with another naturally evolving signed language system. On the other hand, as has been suggested previously (Fernald & Simon, 1984; Masataka, 2000, 2003), the preference for naturally evolving signed languages could also be due to genetic programing.

Nonetheless, the much more noticeable implication of the present results should be the immediate

Table 1 Talairach coordinates and *t* scores of the activated foci identified at each testing

Brain region	Brodmann's area	*x*	*y*	*z*	*t* value
First testing					
Left middle occipital gyrus	19	−44	−78	4	6.58
Second testing					
Right middle frontal gyrus	46	42	17	21	5.26
Left middle frontal gyrus	6, 9	−20	18	51	8.39
Left inferior frontal gyrus	9	−38	7	24	6.98
Left middle temporal gyrus	22	−57	−44	4	5.70
Right superior parietal lobule	40, 7	36	−52	52	6.52
Left superior parietal lobule	7	−34	−61	55	15.4
Left inferior parietal lobule	40	−42	−37	39	5.12
Right middle occipital gyrus	19	24	−87	8	8.48
Left middle occipital gyrus	18, 19	−20	−97	5	7.05
Left cingulated gyrus	24	−8	8	47	10.4
Left pulvinar		−22	−29	3	11.6
Left medial dorsal nucleus		−6	−13	4	7.72

Note. *x*, *y*, *z*, Talairach coordinates.

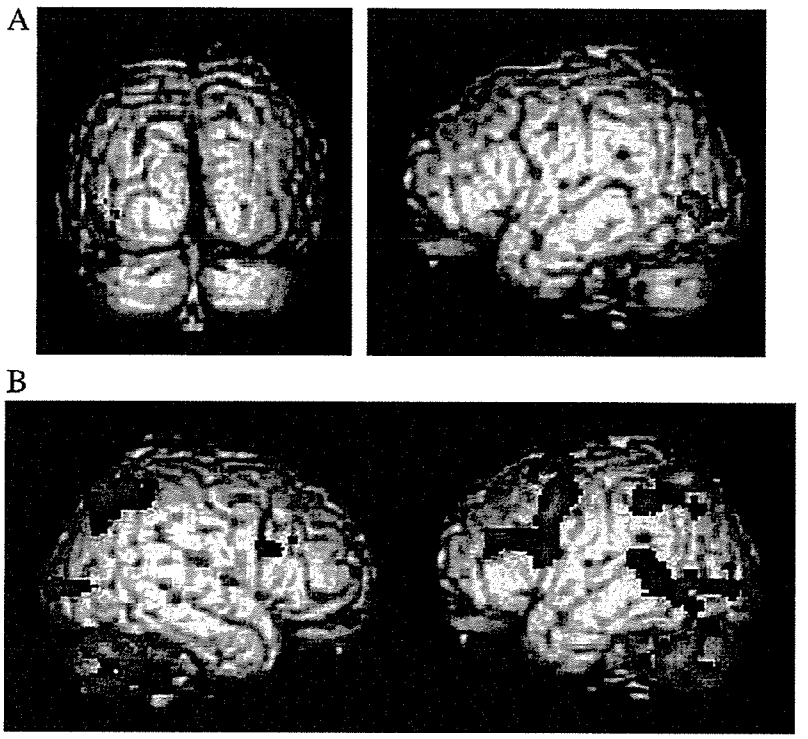

Figure 1 Images showing the regions of activation in each testing (Talairach coordinates of voxels of peak activation: A = first testing, B = second testing).

effects of teaching the participants about ASL signs representing numerals. Significant changes in BOLD activation caused by the learning included increases in the activation level of the left frontal lobe and the bilateral parietal lobes as well as in the left middle temporal gyrus. The temporal gyrus becomes active when picking out the forms of motion of biological entities from other types of motion in the natural environment (Blakemore & Decety, 2001; Frith, 2001). Therefore, the participants should have come to view the ASL signs as meaningful and distinguishable from the control stimuli. Moreover, the frontal and parietal

Table 2 Talairach coordinates and *t* scores of the activated foci whose activation increased from the first to the second testing

Brain region	Brodmann's area	*x*	*y*	*z*	*t* value
Left middle temporal gyrus	22	−57	−44	4	5.55
Right superior parietal lobule	7	34	−52	52	6.82
Left superior parietal lobule	7	−34	−60	51	7.16
Left inferior parietal lobule	40	−42	−48	54	6.01
Left middle frontal gyrus	6, 8	−26	5	61	5.72
Left superior frontal gyrus	6	−10	14	49	5.57
Left precentral gyrus	9	−40	8	36	4.30
Left cingulated gyrus	24	−10	4	48	6.43
Right medial dorsal gyrus		2	−21	7	4.56
Right lateral dorsal gyrus		12	−19	16	4.42

Note. *x*, *y*, *z*, Talairach coordinates.

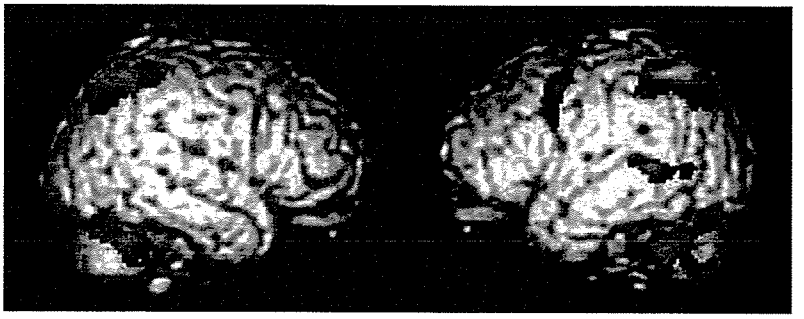

Figure 2 Images showing the regions where activation increased from the first to the second testing.

regions have been reported to be regions that participate in numerical processing (Dehaene, Spelke, Pinel, Stanescus, & Tsivkin, 1999; Piazza & Dehaene, 2005). Obviously, upon learning that the presented signing actions actually have numeric meaning, a network of brain areas that has been previously implicated in numerical processing could immediately become activated. Although behavioral measures were not recorded during the scanning in this experiment, the participants certainly could not decode the numerical meaning of the presented stimuli even after the teaching in spite of the fact that the exact same stimuli were presented repeatedly on the day of the experiment.

Similar findings have recently been reported by Masataka et al. (2005), who conducted a study designed to examine the neuronal correlates of reading Roman numerals and the changes that occur with extensive practice on that task. Hearing participants were scanned by fMRI three times on the first day of the experiment and one last time following 2–3 months of practice on the task, allowing the comparison of brain activations with varying levels of practice given on the same day and across 2–3 months of training. The results of the fMRI measurements revealed that upon learning that these alphabetical symbols actually have numeric meaning, a network of brain areas, many of which have been previously implicated in numerical processing, can be immediately activated. This can occur even though the participants are not yet able to decode the meaning of the presented stimuli at all. Further, although the participants became much more skilled at the decoding after subsequent intensive practice, varying levels of such practice did not affect the pattern of the subsequent activation. Taken together with the results of the study of Masataka, the present findings also confirm the fact that the neural network of brain regions responsible for numerical processing is activated once participants start processing the presented stimuli numerically regardless of whether their attempts are successful.

In all, the network exists on a nonlinguistical basis and functions for the retrieval of arithmetic facts from presented linguistic material regardless of the mode of the language, that is, a region of parietal cortex underlies an abstract-semantic number sense, and a region of left prefrontal cortex underlies more specific operations mediating exact or approximate calculation. Particularly, the fact that linguistic representations of exact numerical values are controlled in the brain's left hemisphere even in native signers should be intriguing. It is well known that spoken language is represented in the brain's left hemisphere. However, much is mysterious about whether the brain sites involved in language processing are determined exclusively by the mechanisms for speaking and hearing, or whether they also involve tissue dedicated to aspects of the patterning of natural language.

Actually, in order to investigate the problem, the existence of naturally evolved signed languages of deaf people has provided a powerful research opportunity because they possess identical levels of linguistic organizations with spoken languages (Klima & Bellugi, 1979). To date, however, available evidence has provoked controversy (Corina, Bavelier, & Neville, 1998; Hickok, Bellugi, & Klima, 1998a). Pioneering lesion studies of brain-damaged deaf adults (Bellugi, Poizner, & Klima, 1989; Hickok, Bellugi, & Klima, 1998b) have shown that deaf signers suffer aphasic symptoms in

signed language following left-hemisphere lesions that are similar to those seen in Broca's and Wernicke's aphasia in hearing patients. Because lasting deficits to signed language processing were not observed after lesions to the right hemisphere, they concluded that the contribution of the right hemisphere may not be central to the processing of natural signed language. Nevertheless, findings from brain-imaging studies, which have been conducted more recently, neither fully concur with this view nor are they consistent across studies. In a large study of Neville and colleagues with the use of fMRI, neural activity was investigated while Deaf and hearing participants processed sentences in ASL and written English (Bavelier et al., 1998; Neville et al., 1998). As the English stimuli, written sentences were presented in 30-s blocks, which alternated with 30-s blocks of consonant strings. As the ASL stimuli, ASL sentences were presented, which alternated with strings of nonsign gestures. At the end of each run, participants were required to decide whether or not specific sentences and nonsense strings had been presented.

When statistical analysis of the MR signal determined which areas of the brain were more active during the language processing blocks, compared to the blocks with nonsense stimuli, elevated activation was found within left-hemisphere structures that are classically linked to language processing for both hearing and deaf native ASL signers. These same areas were also found to be active when English sentences were read by native speakers. Moreover, comparable increase in neural activation was identified in the equivalent areas within the right hemisphere of both deaf and hearing signers. On the other hand, the present results present evidence against such contribution of the right hemisphere with respect to language representation of exact numerical values in the numerical processing at the manual mode by deaf adults.

References

Barth, H., Kanwisher, N., & Spelke, E. (2003). The construction of large number representations in adults. *Cognition, 86,* 201–221.

Barth, H., LaMonto, K., Lipton, J., Dehaene, S., Kanwisher, N., & Spelke, E. (in press). Non-symbolic arithmetic in adults and young children. *Cognition.*

Bavelier, D., Corina, D., Jezzard, P., Clark, V., Karni, A., Lalwani, A., et al. (1998). Hemispheric specialization for English and ASL: Left invariance-right variability. *Neuroreport, 9,* 1537–1542.

Bellugi, U., Poizner, H., & Klima, E. S. (1989). Language, modality and the brain. *Trends in Neurosciences, 12,* 380–388.

Blakemore, S.-J., & Decety, J. (2001). From the perception of action to the understanding of intention. *Nature Reviews Neuroscience, 2,* 561–567.

Brett, M., Johnsrude, I.S., & Owen, A.M. (2002). The problem of functional localization in the human brain. *Nature Reviews Neuroscience, 3,* 243–249.

Corina, D. P., Bavelier, D., & Neville, H. J. (1998). Response. *Trends in Cognitive Sciences, 2,* 468–470.

Dehaene, S. (1997). *The number sense.* Oxford, UK: Oxford University Press.

Dehaene, S., Dupoux, E., & Mehler, J. (1990). Is numerical comparison digital? Analogical and symbolic effects in two-digit number comparison. *Journal of Experimental psychology: Human Perception and Performance, 16,* 626–641.

Dehaene, S., Spelke, E., Pinel, P., Stanescus, R., & Tsivkin, S. (1999). Sources of mathematical thinking: Behavioral and brain-imaging evidence. *Science, 284,* 970–974.

Emmorey, K. (2002). *Language, cognition and the brain: Insights from sign language research.* Mahwah, NJ: Erlbaum.

Fernald, A., & Simon, T. (1984). Expanded intonation contours in mother's speech to newborns. *Developmental Psychology, 20,* 104–113.

Frith, U. (2001). Mind blindness and the brain in autism. *Neuron, 32,* 969–979.

Gallistel, C. R. (1990). *The organization of learning.* Cambridge, MA: MIT Press.

Gallistel, C. R., & Gelman, R. (1992). Preverbal and verbal counting and computation. *Cognition, 44,* 43–74.

Hickok, G., Bellugi, U., & Klima, E. (1998a). What's right about the neural organization of sign language? A perspective on recent neuroimaging results. *Trends in Cognitive Sciences, 2,* 465–468.

Hickok, G., Bellugi, U., & Klima, E. (1998b). The neural organization of language: Evidence from sign language aphasia. *Trends in Cognitive Sciences, 2,* 129–136.

Kobayashi, T., Hiraki, K., Mugitani, R., & Hasegawa, T. (2004). Baby arithmetic: One object plus one tone. *Cognition, 91,* B23–B34.

Klima, E. S., & Bellugi, U. (1979). *The signs of language.* Cambridge, MA: Harvard University Press.

Masataka, N. (2000). The role of modality and input in the earliest stage of language acquisition: Studies of Japanese Sign Language. In C. Chamberlain, J. P. Morford, & R. I. Mayberry (Eds.), *Language acquisition by eye* (pp. 3–24). Hillsdale, NJ: Erlbaum.

Masataka, N. (2003). *The onset of language.* Cambridge: Cambridge University Press.

Masataka, N. (in press). Differences in arithmetic subtraction of non-symbolic numerosities by deaf and hearing adults. *Journal of Deaf Studies and Deaf Education.*

Masataka, N., Ohnishi, T., Imabayashi, E., Hirakata, M., & Matsuda, H. (2005). *Neural correlates for learning to read Roman numerals.* Manuscript in preparation.

McComb, K., Packer, C., & Pusey, A. (1994). Roaring and numerical assessment in contests between groups of female lions, *Panthara leo. Animal Behaviour, 47,* 379–387.

Neville, H. J., Bavelier, D., Corina, D., Rauschecker, J., Karni, A., Lalwani, A., et al. (1998). Cerebral organization for language in deaf and hearing subjects: Biological constraints and effects of experience. *Proceedings of the National Academy of Sciences United States of America, 95,* 922–929.

Ohnishi, T., Matsuda, H., Asada, T, Aruga, M., Hirakata, M., Hishikawa, M., et al. (2001). Functional anatomy of musical perception in musicians. *Cerebral Cortex, 11,* 754–760.

Ohnishi, T., Moriguchi, Y., Matsuda, H., Mori, T., Hirakata, M., Imabayashi, E., et al. (2004). The neural network for the mirror system and the 'theory of mind' in normally developed children: An fMRI Study. *Neuroreport, 15,* 1483–1488.

Padden, C. A. (1988). Grammatical theory and signed languages. In F. Newmayer (Ed.), *Linguistics: The Cambridge survey* (pp. 250–266). Cambridge: Cambridge University Press.

Piazza, M., & Dehaene, S. (2005). From number neurons to mental arithmetic: The cognitive neuroscience of number sense. In M. S. Gazzaniga (Ed.), *The cognitive neurosciences* (3rd ed., pp. 865–875). Cambridge, MA: MIT Press.

Shioda, H. (1985). *Sekai no shuwa* [Signed languages in the world]. Tokyo: Sanseido.

SPM99. (1999). London: Wellcome Department of Cognitive Neurology. Retrieved November 21, 2005 from http://www.fil.ion.ucl.ac.uk/spm.

Suzuki, K., & Kobayashi, T. (2000). Numerical competence in rats (*Rattus norvegicus*): Davis and Bradford (1986) extended. *Journal of Comparative Psychology, 114,* 43–85.

Talairach, J., & Tournoux, P. (1988). *Co-planar streotaxic atlas of the human brain.* Stuttgart: Thieme.

Xu, F., & Spelke, E. (2000). Large number discrimination I 6-month-old infants. *Cognition, 74,* B1–B11.

Received July 5, 2005; revisions received October 21, 2005; accepted October 24, 2005.

Available online at www.sciencedirect.com
SCIENCE DIRECT®
Biochemical and Biophysical Research Communications 345 (2006) 904–909
BBRC
www.elsevier.com/locate/ybbrc

Hyperactivation of midbrain dopaminergic system in schizophrenia could be attributed to the down-regulation of dysbindin

Natsuko Kumamoto [a,b,1], Shinsuke Matsuzaki [a,b,c,*,1], Kiyoshi Inoue [a,b], Tsuyoshi Hattori [a,b], Shoko Shimizu [a,b], Ryota Hashimoto [c,d,e], Atsushi Yamatodani [f], Taiichi Katayama [g], Masaya Tohyama [a,b,c]

[a] *Department of Anatomy and Neuroscience, Graduate School of Medicine, Osaka University, 2-2 Yamadaoka, Suita, Osaka 565-0871, Japan*
[b] *The 21st Century COE program, 2-2 Yamadaoka, Suita, Osaka 565-0871, Japan*
[c] *The Osaka-Hamamatsu Joint Research Center for Child Mental Development, Osaka 565-0871, Japan*
[d] *Department of Psychiatry, Osaka University Graduate school of Medicine, 2-2 Yamadaoka, Suita, Osaka 565-0871, Japan*
[e] *Department of Mental Disorder Research, National Institute of Neuroscience, National Center of Neurology and Psychiatry, 4-1-1 Ogawahigashicho, Kodaira, Tokyo 187-8502, Japan*
[f] *Department of Bioinformatics, Graduate School of Allied Health Sciences, Faculty of Medicine, Osaka University, Osaka, Japan*
[g] *Department of Anatomy and Neuroscience, Hamamatsu University School of Medicine, 1-20-1 Handayama, Hamamatsu, Shizuoka 431-3192, Japan*

Received 18 April 2006
Available online 6 May 2006

Abstract

Extraordinal activation of nigrostriatal and mesolimbic dopaminergic systems (midbrain dopaminergic system) is thought to be one of the most important etiologies for schizophrenia, though the reason why unusual hyperactivation of the dopaminergic system occurs in the schizophrenic brain is quite obscure. Dysbindin, one of the most susceptible genes for schizophrenia, has been reported to be reduced in the schizophrenic brain. In situ hybridization analysis showed the mRNA expression of dysbindin in the mouse substantia nigra. Furthermore, suppression of dysbindin expression in PC12 cells resulted in an increase of the expression of SNAP25, which plays an important role in neurotransmitter release, and increased the release of dopamine. On the other hand, up-regulation of dysbindin expression in PC12 cells showed a tendency to decrease the expression of SNAP25. These data suggest that dysbindin might regulate the dopamine release of the dopaminergic system via modulation of the expression of SNAP25.

Keywords: Schizophrenia; Dysbindin; Dopamine; SNAP25; PC12

Schizophrenia is a devastating psychiatric disorder with a lifetime prevalence of about 1% worldwide, which commonly leads to a chronic course. As to the etiology of schizophrenia, little is known at the molecular level. As a possible pathophysiology, unusual neurotransmissions such as dopaminergic and glutamatergic systems have been suggested for the mechanism of symptoms for schizophrenia [1–7]. Furthermore, it has been agreed that acceleration of dopaminergic systems is closely related to expression of psychotic symptoms. In support of this, antipsychotic drugs work via their action on dopaminergic receptors [1,2] and dopamine-enhancing drugs mimic psychotic symptoms [3,4]. However, underlying molecular mechanism why dopaminergic systems are accelerated in the schizophrenia is still unclear.

On the other hand, several lines of studies have revealed that schizophrenia is a multifactorial disorder influenced by genetic, neurodevelopmental, and social factors [8,9]. In particular, it has been reported that chromosome 6p is one of the most susceptible regions in linkage studies of

* Corresponding author. Fax: +81 6 6879 3229.
E-mail address: s-matsuzaki@anat2.med.osaka-u.ac.jp (S. Matsuzaki).
[1] These authors contributed equally to this work.

0006-291X/$ - see front matter © 2006 Elsevier Inc. All rights reserved.
doi:10.1016/j.bbrc.2006.04.163

schizophrenia [10,11]. Genetic variants in a gene on 6p22.3, dysbindin (DTNBP1), which is identified as a protein interacting with dystrobrevins [12], have been shown to be associated with schizophrenia [13]. Since then, many reports support the etiological relation between dysbindin and schizophrenia [14–24]. However, precise pathophysiology of schizophrenia on molecular level is still quite unclear. Attracting our particular interest is that a recent report showed that expression of dysbindin mRNA tends to be decreased in the substantia nigra in the brain of patients with schizophrenia [25], suggesting the physiological interaction between decrease in dysbindin and increase in dopaminergic transmission in the schizophrenia.

As for neurotransmitter release, SNAP25, which is a component of stable SNARE (soluble NSF attachment protein receptors) core complex and relates to the synaptic vesicle membrane docking and fusion pathway [26–28], is involved in schizophrenia; the alteration of SNAP25 expression level in schizophrenia has been reported in many studies [29–35]. A previous study showed that down-regulation of dysbindin in cortex primary cultures, mostly glutamatergic neurons, resulted in reduction of SNAP25 expression and glutamatergic release [14]. However, involvement of dysbindin in dopaminergic release has not been reported yet. In this paper, we examined the effect of dysbindin on SNAP25 expression and dopaminergic release in dopaminergic cells.

Materials and methods

In situ hybridization. The template cDNA for probes (the sequence corresponding to nucleotides 39–1289 of mouse Dysbindin, GenBank Accession No. NM_025772) was subcloned into pGEM-T vector (Promega, Madison, WI, USA). ^{35}S-labeled RNA probes were synthesized by in vitro transcription using T7 and SP6 RNA polymerase. In addition, the sense probes were synthesized as negative controls. For the ^{35}S-labeled probes, brains of adult male C57/BL6 mice were freshly frozen and 14 μm cryosections were fixed in 4% formaldehyde in 0.1 M phosphate buffer (PB) pH 7.4, treated with proteinase K (10 μg/ml) for 3 min, and postfixed in the same fixative, acetylated with acetic anhydride, dehydrated in ascending alcohol series, and air-dried. The sections were incubated for 12 h at 55 °C in hybridization buffer (50% formamide, 0.3 M NaCl, 20 mM Tris–HCl, 10% dextran sulfate, 1× Denhardt's solution, 500 μg/ml yeast tRNA, 20 mM dithiothreitol, and 200 μg/ml salmon testis DNA) containing one of the ^{35}S-labeled cRNA probes. After hybridization, sections were washed with 50% formamide/2× standard sodium citrate (SSC) at 65 °C and incubated with 1 μg/ml RNaseA in RNase buffer (0.5 M NaCl, 10 mM Tris–HCl, and 1 mM EDTA, pH 8.0) for 30 min at 37 °C. After rinsing with RNase buffer, sections were washed in 50% formamide/2× SSC at 65 °C, rinsed with 2× SSC and 0.1× SSC, dehydrated in alcohol, and air-dried. The slides were exposed to Kodak Bio-Max MR film for 1 week. Films were developed, and black and white images of mRNA expression were obtained. The slides were then counterstained with thionine. The film autoradiograph and the thionine-stained sections were captured by a scanner (Epson, Tokyo, Japan) and a CCD camera (OLYMPUS, Tokyo, Japan) connected with a stereomicroscope (Carl Zeiss, Oberkochen, Germany), respectively.

Cell culture. PC12 cells were plated in tissue culture dishes precoated with Cellmatrix TypeIV (Nitta Gelatin, Osaka, Japan) and maintained in Dulbecco's modified Eagle's medium (Invitrogen, Carlsbad, CA, USA) supplemented with 5% FBS, 10% heat-inactivated horse serum, and antibiotics in 5% CO_2 atmosphere at 37 °C.

Plasmids and electropolation. Full-length human dysbindin cDNA (GenBank Accession No. AF394226) was cloned into pEGFP-C1 vector (Clontech, Palo Alto, CA, USA) and an empty pGFP-C1 vector was used as negative control. 6×10^6 PC12 cells were used in each transfection experiment with the Nucleofector™ (Amaxa Biosystems, Cologne, Germany). Cells were spun down at 90 g for 5 min, and the medium was removed. Then they were re-suspended in 100 μl Nucleofector™ solutionV (Amaxa Biosystems) at room temperature followed by addition of 2 μg of vectors. The mixture was transferred to a 2 mm electropolation cuvette (Amaxa Biosystems) inserted in the Nucleofector™ and program U-29 was used for transfecting the cells. Immediately after transfection, 500 μl of culture medium was added to the cuvette and the sample transferred into collagen-coated 6-well plates with 2 ml culture medium in each well. After transfection, the cells were cultured for additional 24 h and then subjected to Western blot analysis or dopamine secretion assays.

siRNA design and RNA interference. To inhibit Dysbindin synthesis, we used 5′-AAGUGACAAGUCAAGAGAA-3′ siRNA, the sequence of which is corresponding to nucleotides 175–197 of human Dysbindin mRNA. Scrambled siRNA 5′-UUCUCUUGACUUGUCACUU-3′, the target of which is not present in mammalian cells, was used as a negative control. Both sense and antisense strands with two base overhangs were synthesized by NIPPON-EGT (Toyama, Japan) in desalted form. Transfection of both siRNAs was carried out using Lipofectamine2000 (Invitrogen) according to manufacturer's protocol. To transfect the siRNA to the cells, 500 μl Opti-MEM (Invitrogen), 5 μl Lipofectamine2000, and 250 pmol siRNA per well were used. After transfection, the cells were cultured for 72 h and then subjected to Western blot analysis or dopamine secretion assays.

Antibodies. Polyclonal anti-dysbindin antibody was produced as described previously [36]. Briefly, the peptide synthesized (QSDEEEVQVDTALC: 320–333 amino acid residue of human dysbindin, with no homology in any mammalian protein) was conjugated with maleimide-activated keyhole limpet hemocyanin and immunized to two rabbits. The titer was measured by ELISA and sera of high titer against the peptide were obtained from both rabbits. The sera were affinity purified by a column conjugated with the immunized peptide. Monoclonal anti-GFP antibody (Santa Cruz Biotechnology, Santa Cruz, CA, USA), monoclonal anti-β-actin antibody (Chemicon, Temecula, CA, USA), and monoclonal anti-SNAP25 antibody (BD Transduction Laboratories, Lexington, KY) were used in Western blot analysis.

Western blot analysis. PC12 cells were collected after washing with PBS and lysed in TNE buffer (20 mM Tris–HCl, pH 7.5, 150 mM NaCl, and 1 mM EDTA) containing 1% NP-40 and protease inhibitor cocktail (Roche, Sydney, Australia), incubated on ice for 30 min, and centrifuged at 15000*g* for 30 min. Lysates were boiled with SDS sample buffer (0.125 M Tris–HCl, pH 6.8, 10% 2-mercaptoethanol, 4% SDS, 10% sucrose, and 0.004% bromophenol blue) for 5 min and subjected to SDS–PAGE. The proteins were transferred onto PVDF membranes and blocked for 30 min at room temperature in PBS containing 5% BSA and 0.05% Tween 20. Membranes were blotted overnight at 4 °C with polyclonal anti-dysbindin antibody (1:500), monoclonal anti-GFP antibody (1:1000), monoclonal anti-β-actin antibody (1:1000), and monoclonal anti-SNAP25 antibody (1:500). The membranes were then incubated for 1 h at room temperature with anti-rabbit or anti-mouse IgG HRP-linked antibody, respectively (1:10000; Cell signaling Technology, Beverly, MA, USA). Immunoblotting was visualized by chemiluminescence using the ECL kit (Amersham Biosciences, Buckinghamshire, UK). The immunoblotting experiments were performed at least three times and they were quantitatively analyzed by capturing images on films using a scanner (Epson, Tokyo, Japan) in conjunction with the ImageJ software (version 1.34s, National Institutes of Health, USA). The data were expressed as means ± SEM for at least three independent experiments. Statistical analysis was performed by Students' *t*-test. *p*-values reported are two tailed.

Dopamine secretion assay. PC12 cells grown on collagen-coated 6-well plates were washed with 2 ml of basal medium containing 150 mM NaCl, 5 mM KCl, 2 mM $CaCl_2$, 10 mM Hepes, and pH adjusted to 7.4 with NaOH and subsequently incubated for 15 min in basal medium as basal

secretion or high potassium medium containing 100 mM NaCl, 50 mM KCl, 2 mM $CaCl_2$, 10 mM Hepes, and pH adjusted to 7.4 with NaOH as stimulated secretion.

To determine 'released dopamine', 1/100 volume of 0.2 M EDTA-2Na, 0.2 M $Na_2S_2O_5$ and 1/30 volume of 60% perchloric acid were added to the collected medium. To determine 'intracellular dopamine' after harvesting the medium, the attached cells were extracted with 2% perchloric acid containing 2 mM EDTA-2Na and 2 mM $Na_2S_2O_5$. Both samples were centrifuged at 12,000*g* for 30 min at 4 °C. Dopamine levels in 500 μl of the supernatant were determined in a fully automated HPLC-fluorometric system (Model HLC-725CA Catecholamine Analyzer, Tosoh, Tokyo, Japan) using the diphenylethylenediamine condensation method [37]. The amount of dopamine released in the medium is defined as 'released dopamine', and the amount of dopamine in cells after releasing of dopamine is defined as 'intracellular dopamine'. 'Total dopamine', 'basal dopamine secretion ratio', 'evoked dopamine secretion ratio', and 'accelerated dopamine release ratio' are defined as follows.

'Total dopamine' = 'released dopamine' + 'intracellular dopamine'.
'Basal dopamine secretion ratio' = 'released dopamine' in the low K^+ medium/'total dopamine' in the low K^+ medium.
'Evoked dopamine secretion ratio' = 'released dopamine' in the high K^+ medium/'total dopamine' in the high K^+ medium.
'Accelerated dopamine release ratio' = 'evoked dopamine secretion ratio'/'basal dopamine secretion ratio'.

The data were expressed as means ± SEM for at least three independent experiments. Statistical analysis was performed by Students' *t*-test. *p*-values reported are two tailed.

Results

Localization of dysbindin with special reference to the coexistence of dopamine in the substantia nigra

If dysbindin is related to dopamine release, it is likely that dysbindin is localized in the dopaminergic neurons. Previous reports showed the presence of dysbindin mRNA in substantia nigra where there is a huge collection of dopaminergic neurons in human brain [25] and the presence of dysbindin protein in substantia nigra in rodent brain [12]. Thus, we confirmed whether the dysbindin mRNA is expressed in rodent brain, especially in midbrain. As a result of in situ hybridization analysis, the dysbindin mRNA was detected in rat and mouse brains (data not shown), and the expression of dysbindin mRNA in substantia nigra pars compacta was confirmed in mouse as same as in human (Fig. 1). This result suggests the possibility of the functional involvement of dysbindin in midbrain dopaminergic systems.

Dysbindin effects on SNAP25 expression level in PC12 cells

To disclose the effects of dysbindin on dopaminergic neurons, we used clonal rat pheochromocytoma (PC12) cells as a tool for in vitro analysis, which synthesize, store, and release dopamine in a similar manner as neurons [38]. The expression of dysbindin mRNA and protein in PC12 cells was confirmed using RT-PCR and Western blot analysis (data not shown). As recent report showed that dysbindin regulated neurotransmitter release (glutamate) via SNAP25 expression in primary cultures, mostly glutamatergic neurons [14], we examined the effect of dysbindin expression level on SNAP25 expression in PC12 cells. To knockdown the expression of dysbindin in PC12 cells, we performed lipofection of siRNA for dysbindin. We quantified SNAP25 and β-actin proteins when we succeeded to suppress the dysbindin protein expression (approximately 50% reduction compared with control condition). As shown in Fig. 2a, SNAP25 protein expression was increased by 34% in dysbindin knockdown cells without alteration of β-actin protein expression. We also quantified SNAP25 and β-actin proteins when dysbindin was overexpressed by transfection of GFP-tagged human dysbindin in PC12 cells. GFP-tagged human dysbindin was detected by anti-GFP antibody (Fig. 2b) and by anti-dysbindin antibody (data not shown). The expression level of SNAP25 and β-actin did not significantly change in dysbindin-overexpressed PC12 cells (Fig. 2b). These findings suggest a possible regulation of SNAP25 expression by dysbindin in dopaminergic cells.

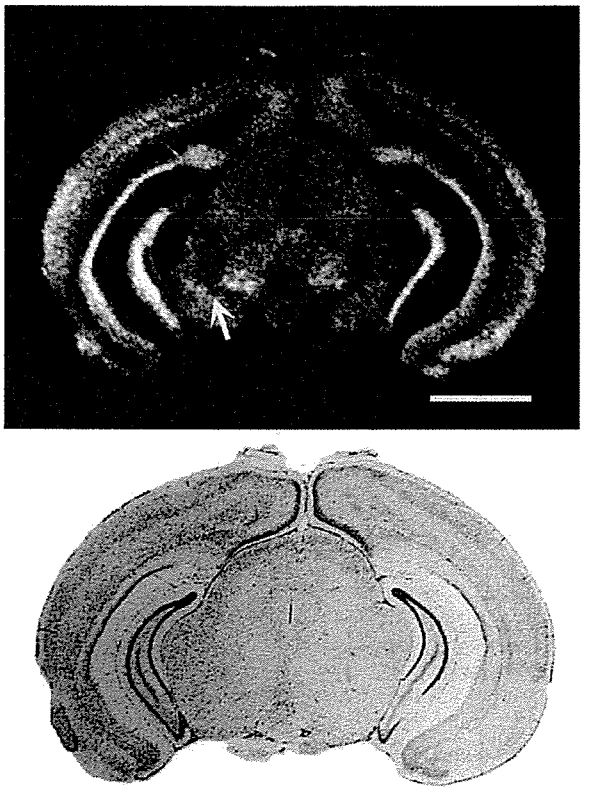

Fig. 1. Expression pattern of dysbindin mRNA in the adult mouse midbrain. Film autoradiographs of in situ hybridization on coronal brain sections with ^{35}S-labeled probes (upper panel) show the signal of dysbindin mRNA in the substantia nigra pars compacta (arrow). The same sections were stained by thionine and identified exact brain region (lower panel). Scale bar; 2 mm.

Functional interaction between dysbindin and dopamine

To evaluate functions of dysbindin in dopaminergic cells, we examined the effect of dysbindin on dopaminergic

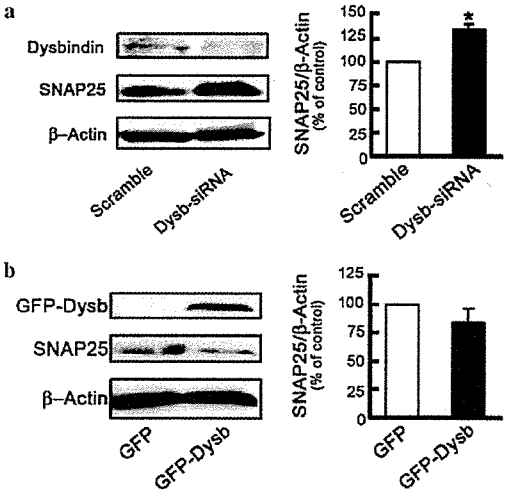

Fig. 2. Western blotting of the lysates of dysbindin-knockdown and dysbindin-overexpressed PC 12 cells. (a) Western blotting of the lysates of dysbindin-knockdown PC12 cells. PC12 cells were treated with dysbindin-siRNA (Dys-siRNA; 100 nM) or scramble-siRNA (Scramble; 100 nM) for 72 h and collected. Lysates were immunoblotted with anti-dysbindin antibody (top panel), anti-SNAP25 antibody (middle panel), and anti-β-actin antibody (bottom panel). Data are shown as a percentage of the control group. Data represent means ± SEM ($n = 3$). $^*p < 0.01$ compared with control (Scramble). (b) Western blotting of the lysates of dysbindin-overexpressed PC12 cells. Cells were transfected with GFP or GFP-dysbindin (GFP-Dys) with the Nucleofector™. Cell lysates were collected 24 h after the transfection and immunoblotted with anti-GFP antibody (top panel), anti-SNAP25 antibody (middle panel), and anti-β-actin antibody (bottom panel). Data represent means ± SEM compared with control (GFP) ($n = 3$).

release using dysbindin-knockdown or overexpressed PC12 cells As shown in Fig. 3a, knockdown of dysbindin in PC12 cells, which caused an increase of SNAP25 protein as described above, did not affect the basal dopamine secretion ratio, however, accelerated dopamine secretion ratio was significantly increased (Fig. 3b). To examine whether dysbindin has an effect on dopamine synthesis in PC12 cells, we measured the amount of total dopamine in dysbindin-knockdown PC12 cells. No significant change of total dopamine level was observed (Fig. 3c). Then we investigated the effect of overexpression of dysbindin in PC12 cells, which reduce the SNAP25 expression, on dopamine release and dopamine synthesis. The basal dopamine secretion ratio of PC12 cells was not affected by overexpression of dysbindin (Fig. 3d), and the accelerated dopamine secretion ratio of PC12 cells tended to be decreased (11%) by overexpression of dysbindin, but not significant ($p = 0.079$) as compared with control (GFP-overexpressed) cells (Fig. 3e). Total dopamine in dysbindin-overexpressed PC12 cells was measured, but no significant change of total dopamine level was observed (Fig. 3f). These results suggest that the endogenous dysbindin protein has an inhibiting effect on dopaminergic release in neurons but is unlikely to have direct implication with dopamine synthesis.

Discussion

In this study, we showed that suppression of dysbindin expression in PC12 cells resulted in an increase of the

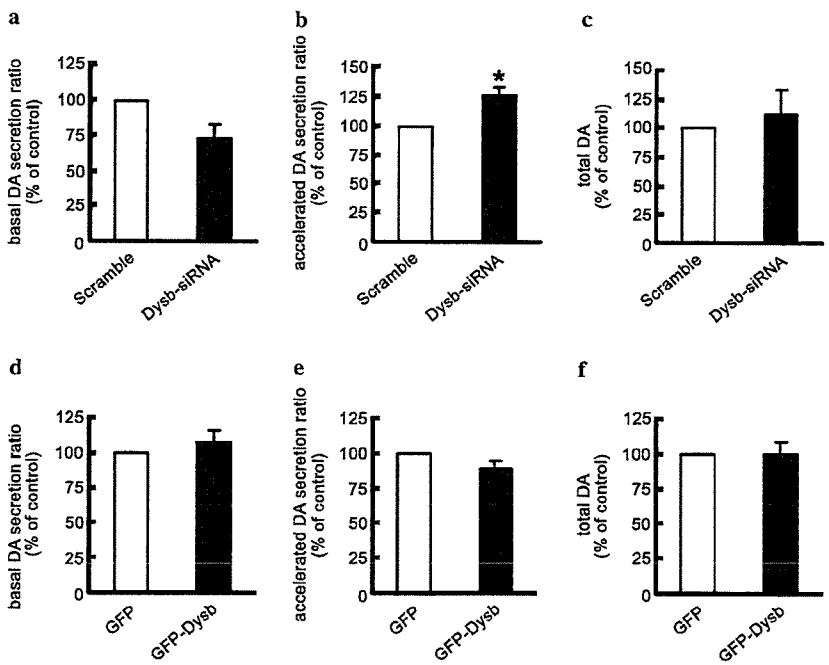

Fig. 3. Effect of dysbindin on dopaminergic release in PC12 cells. (a–c) Data of dysbindin-knockdown PC12 cells. Data are shown as a percentage of the control group. Data represent means ± SD ($n = 3$). $^*p < 0.05$ compared with control (Scramble). (d–f) Data of dysbindin-overexpressed PC12 cells. Data are shown as a percentage of the control group. Data represent means ± SEM ($n = 4$). Dopamine levels were determined as described in Materials and methods. (a,d) The basal dopamine (DA) secretion ratio, (b,e) the accelerated dopamine secretion, and (c,f) total dopamine.

expression of SNAP25. In dysbindin-knockdown PC12 cells, the accelerated dopamine secretion ratio increased, however, the basal dopamine secretion ratio did not, suggesting that dysbindin inhibits the dopaminergic release under the high K^+ stimulation in dopaminergic cells. SNAP25 induces Ca^{2+}-dependent secretion and a recent report showed that SNAP25 knockout mice eliminated stimulus-evoked neurotransmitter release, but not spontaneous neurotransmitter release [39]. The findings seem not to conflict with our results and to support the possibility that dysbindin might regulate the dopamine release of the dopaminergic systems via modulation of the expression of SNAP25. A previous study reported that in mouse mutant coloboma (*Cm/+*), which expresses only 50% of normal SNAP25 protein concentration throughout the brain, there are no significant differences in basal release of dopamine, but KCl-induced release of dopamine was blocked in dorsal striatum [40], suggesting the functional implication of SNAP25 on dopaminergic systems. As dysbindin mRNA was tended to be decreased in the substantia nigra in the brain of schizophrenia [25], it is likely that reduction of the dysbindin protein leads to the increase of SNAP25 and up-regulation of SNAP25 activates the dopaminergic transmission to increase the dopamine release. On the other hand, our data showed dysbindin did not alter the total dopamine level in PC12 cells, suggesting dysbindin is unlikely to have direct implication on dopamine synthesis. To elucidate the function of dysbindin in dopaminergic cells, further investigations into details of dopamine dynamics, such as metabolism and turn over, are required.

In addition to dopaminergic system, involvement of dysbindin in glutamatergic system has been reported [14,41]. The interaction between dopaminergic systems and glutamatergic systems has reported in many studies [42]. NMDA hypofunction causes hyperstimulation of striatal D2 receptors and D2 stimulation decreases NMDA transmission in corticostriatal glutamatergic tracts. Interestingly, a present report showed that down-regulation of dysbindin in cortex primary cultures resulted in reduction of SNAP25 expression and glutamatergic release [14]. These results seem to be the opposite of our data. However, if dysbindin acted on both glutamatergic systems in cortex and dopaminergic systems in midbrain, both hypoglutamatergic states and hyperdopaminergic states could be explained by reduction of dysbindin in schizophrenic brain, that is very compatible with the pathophysiology of schizophrenia, and that suggests the possibility that dopamine/glutamate positive feedback loops may be enhanced by the reduced expression of dysbindin in cortex and midbrain of schizophrenia patients. We need more consideration to elucidate the effects of dysbindin on dopaminergic and glutamatergic transmissions.

Acknowledgments

We thank Ms. Arakawa, Ms. Moriya, and Ms. Ohashi for preparing for our experiments and acknowledge Mr. Taniguchi and Mr. Koyama for their excellent technical expertise.

References

[1] P. Seeman, T. Lee, Antipsychotic drugs: direct correlation between clinical potency and presynaptic action on dopamine neurons, Science 188 (1975) 1217–1219.
[2] I. Creese, D.R. Burt, S.H. Snyder, Dopamine receptor binding predicts clinical and pharmacological potencies of antischizophrenic drugs, Science 192 (1976) 481–483.
[3] J.A. Lieberman, J.M. Kane, J. Alvir, Provocative tests with psychostimulant drugs in schizophrenia, Psychopharmacology (Berl) 91 (1987) 415–433.
[4] B. Angrist, D.P. Van Kammen, CNS stimulants as tools in the study of schizophrenia, Trends Neurosci. 7 (1984) 388–390.
[5] C.A. Tamminga, H.H. Holcomb, X.M. Gao, A.C. Lahti, Glutamate pharmacology and the treatment of schizophrenia: current status and future directions, Int. Clin. Psychopharmacol. 10 (Suppl. 3) (1995) 29–37.
[6] D.C. Goff, J.T. Coyle, The emerging role of glutamate in the pathophysiology and treatment of schizophrenia, Am. J. Psychiatry 158 (2001) 1367–1377.
[7] J.D. Jentsch, R.H. Roth, The neuropsychopharmacology of phencyclidine: from NMDA receptor hypofunction to the dopamine hypothesis of schizophrenia, Neuropsychopharmacology 20 (1999) 201–225.
[8] M.J. Owen, Genomic approaches to schizophrenia, Clin. Ther. 27 (2005) S2–S7.
[9] D.R. Weinberger, Genetics mechanisms of psychosis: in vivo and postmortern genomics, Clin. Ther. 27 (2005) S8–S15.
[10] S. Wang, C.E. Sun, C.A. Walczak, J.S. Ziegle, B.R. Kipps, L.R. Goldin, S.R. Diehl, Evidence for a susceptibility locus for schizophrenia on chromosome 6pter-p22, Nat. Genet. 10 (1995) 41–46.
[11] R.E. Straub, C.J. MacLean, F.A. O'Neill, J. Burke, B. Murphy, F. Duke, R. Shinkwin, B.T. Webb, J. Zhang, D. Walsh, K.S. Kendler, A potential vulnerability locus for schizophrenia on chromosome 6p24-22: evidence for genetic heterogeneity, Nat. Genet. 11 (1995) 287–293.
[12] M.A. Benson, S.E. Newey, E. Martin-Rendon, R. Hawkes, D.J. Blake, Dysbindin, a novel coiled-coil-containing protein that interacts with the dystrobrevins in muscle and brain, J. Biol. Chem. 276 (2001) 24232–24241.
[13] R.E. Straub, Y. Jiang, C.J. MacLean, Y. Ma, B.T. Webb, M.V. Myakishev, C. Harris-Kerr, B. Wormley, H. Sadek, B. Kadambi, A.J. Cerare, A. Gibberman, X. Wang, F.A. O'Neill, D. Walsh, K.S. Kendler, Genetic variation in the 6p22.3 gene DTNBP1, the human ortholog of the mouse dysbindin gene, is associated with schizophrenia, Am. J. Hum. Genet. 71 (2002) 337–348.
[14] T. Numakawa, Y. Yagasaki, T. Ishimoto, T. Okada, T. Suzuki, N. Iwata, N. Ozaki, T. Taguchi, M. Tatsumi, K. Kamijima, R.E. Straub, D.R. Weinberger, H. Kunugi, R. Hashimoto, Evidence of novel neuronal functions of dysbindin, a susceptibility gene for schizophrenia, Hum. Mol. Genet. 13 (2004) 2699–2708.
[15] A.H. Fanous, E.J. van den Oord, B.P. Riley, S.H. Aggen, M.C. Neale, F.A. O'Neill, D. Walsh, K.S. Kendler, Relationship between a high-risk haplotype in the DTNBP1 (dysbindin) gene and clinical features of schizophrenia, Am. J. Psychiatry 162 (2005) 1824–1832.
[16] N.J. Bray, A. Preece, N.M. Williams, V. Moskvina, P.R. Buckland, M.J. Owen, M.C. O'Donovan, Haplotypes at the dystrobrevin binding protein 1 (DTNBP1) gene locus mediate risk for schizophrenia through reduced DTNBP1 expression, Hum. Mol. Genet. 14 (2005) 1947–1954.
[17] M.C. Gornick, A.M. Addington, A. Sporn, N. Gogtay, D. Greenstein, M. Lenane, P. Gochman, A. Ordonez, R. Balkissoon, R. Vakkalanka, D.R. Weinberger, J.L. Rapoport, R.E. Straub, Dysbindin (DTNBP1, 6p22.3) is associated with childhood-onset psychosis

and endophenotypes measured by the premorbid adjustment scale (PAS), J. Autism. Dev. Disord. 10 (2005) 1–8.
[18] A. Van Den Bogaert, J. Schumacher, T.G. Schulze, A.C. Otte, S. Ohlraun, S. Kovalenko, T. Becker, J. Freudenberg, E.G. Jonsson, M. Mattila-Evenden, G.C. Sedvall, P.M. Czerski, P. Kapelski, J. Hauser, W. Maier, M. Rietschel, P. Propping, M.M. Nothen, S. Cichon, The DTNBP1 (dysbindin) gene contributes to schizophrenia, depending on family history of the disease, Am. J. Hum. Genet. 73 (2003) 1438–1443.
[19] S.G. Schwab, M. Knapp, S. Mondabon, J. Hallmayer, M. Borrmann-Hassenbach, M. Albus, B. Lerer, M. Rietschel, M. Trixler, W. Maier, D.B. Weinberger, Support for association of schizophrenia with genetic variation in the 6p22.3 gene, dysbindin, in sib-pair families with linkage and in an additional sample of triad families, Am. J. Hum. Genet. 72 (2003) 185–190.
[20] B. Funke, C.T. Finn, A.M. Plocik, S. Lake, P. DeRosse, J.M. Kane, R. Kucherlapati, A.K. Malhotra, Association of the DTNBP1 locus with schizophrenia in a U.S. population, Am. J. Hum. Genet. 75 (2004) 891–898.
[21] N.M. Williams, A. Preece, D.W. Morris, G. Spurlock, N.J. Bray, M. Stephens, N. Norton, H. Williams, M. Clement, S. Dwyer, C. Curran, J. Wilkinson, V. Moskvina, J.L. Waddington, M. Gill, A.P. Corvin, S. Zammit, G. Kirov, M.J. Owen, M.C. O'Donovan, Identification in 2 independent samples of a novel schizophrenia risk haplotype of the dystrobrevin binding protein gene (DTNBP1), Arch. Gen. Psychiatry 61 (2004) 336–344.
[22] G. Kirov, D. Ivanov, N.M. Williams, A. Preece, I. Nikolov, R. Milev, S. Koleva, A. Dimitrova, D. Toncheva, M.C. O'Donovan, M.J. Owen, Strong evidence for association between the dystrobrevin binding protein 1 gene(DTNBP1) and schizophrenia in 488 parent-offspring trios from Bulgaria, Biol. Psychiatry 55 (2004) 971–975.
[23] J.X. Tang, J. Zhou, J.B. Fan, X.W. Li, Y.Y. Shi, N.F. Gu, G.Y. Feng, Y.L. Xing, J.G. Shi, L. He, Family-based association study of DTNBP1 in 6p22.3 and schizophrenia, Mol. Psychiatry 8 (2003) 717–718.
[24] E.J. van den Oord, P.F. Sullivan, Y. Jiang, D. Walsh, F.A. O'Neill, K.S. Kendler, B.P. Riley, Identification of a high-risk haplotype for the dystrobrevin binding protein 1(DTNBP1) gene in the Irish study of high-density schizophrenia families, Mol. Psychiatry 8 (2003) 499–510.
[25] C.S. Weickert, R.E. Straub, B.W. McClintock, M. Matsumoto, R. Hashimoto, T.M. Hyde, M.M. Herman, D.R. Weinberger, J.E. Kleinman, Human dysbindin (DTNBP1) gene expression in normal brain and in schizophrenic prefrontal cortex and midbrain, Arch. Gen. Psychiatry 61 (2004) 544–555.
[26] M. Bajjalieh, R.H. Scheller, The biochemistry of neurotransmitter secretion, J. Biol. Chem. 270 (1995) 1971–1974.
[27] A. Hodel, Snap-25, Int. J. Biochem. Cell Biol. 30 (1998) 1069–1073.
[28] G.A. Oyler, G.A. Higgins, R.A. Hart, E. Battenberg, M. Billingsley, F.E. Bloom, M.C. Wilson, The identification of a novel synaptosomal-associated protein, SNAP-25, differentially expressed by neuronal subpopulations, J. Cell Biol. 109 (1989) 3039–3052.
[29] G. Honer, P. Falkai, T.A. Bayer, J. Xie, L. Hu, H.Y. Li, V. Arango, J.J. Mann, A.J. Dwork, W.S. Trimble, Abnormalities of SNARE mechanism proteins in anterior frontal cortex in severe mental illness, Cereb. Cortex 12 (2002) 349–356.
[30] C.N. Karson, R.E. Mrak, K.O. Schluterman, W.Q. Sturner, J.G. Sheng, W.S. Griffin, Alterations in synaptic proteins and their encoding mRNAs in prefrontal cortex in schizophrenia: a possible neurochemical basis for 'hypofrontality', Mol. Psychiatry 4 (1999) 39–45.
[31] E.B. Mukaetova-Ladinska, J. Hurt, W.G. Honer, C.R. Harrington, C.M. Wischik, Loss of synaptic but not cytoskeletal proteins in the cerebellum of chronic schizophrenics, Neurosci. Lett. 317 (2002) 161–165.
[32] M. Thompson, S. Egbufoama, M.P. Vawter, SNAP-25 reduction in the hippocampus of patients with schizophrenia, Prog. Neuropsychopharmacol. Biol. Psychiatry 27 (2003) 411–417.
[33] P.M. Thompson, M. Kelley, J. Yao, G. Tsai, D.P. van Kammen, Elevated cerebrospinal fluid SNAP-25 in schizophrenia, Biol. Psychiatry 53 (2003) 1132–1137.
[34] P.M. Thompson, C. Rosenberger, C. Qualls, CSF SNAP-25 in schizophrenia and bipolar illness. A pilot study, Neuropsychopharmacology 21 (1999) 717–722.
[35] P.M. Thompson, A.C. Sower, N.I. Perrone-Bizzozero, Altered levels of the synaptosomal associated protein SNAP-25 in schizophrenia, Biol. Psychiatry 43 (1998) 239–243.
[36] R. Hashimoto, Y. Numakawa, S. Komai, Y. Kashiwagi, K. Tamura, T. Goto, S. Aimoto, K. Kaibuchi, S. Shiosaka, M. Takeda, Site-specific phosphorylation of neurofilamine-L is mediated by calcium/calmodulin-dependent protein kinase II in the apical dendrites during long-term potentiation, J. Neurochem. 75 (2000) 373–382.
[37] H. Nohta, A. Mitui, Y. Ohkura, Spectrofluorimetric determination of catecholamines with 1,2-diphenylethylenediamine, Anal. Chim. Acta 165 (1984) 171–176.
[38] L.A. Greene, G. Rein, Release, storage and uptake of catecholamines by a clonal cell line of nerve growth factor (NGF) responsive pheochromocytoma cells, Brain Res. 129 (1997) 247–263.
[39] P. Washbourne, P.M. Thompson, M. Carta, E.T. Costa, J.R. Mathews, G. Lopez-Bendito, Z. Molnar, M.W. Becher, C.F. Valenzuela, L.D. Partridge, M.C. Wilson, Genetic ablation of the t-SNARE SNAP-25 distinguishes mechanisms of neuroexocytosis, Nat. Neurosci. 5 (2002) 19–26.
[40] J. Raber, P.P. Mehta, M. Kreifeldt, L.H. Parsons, F. Weiss, F.E. Bloom, M.C. Wilson, Coloboma hyperactive mutant mice exhibit regional and transmitter-specific deficits in neurotransmission, J. Neurochem. 68 (1) (1997) 176–186.
[41] K. Talbot, W.L. Eidem, C.L. Tinsley, M.A. Benson, E.W. Thompson, R.J. Smith, C.G. Hahn, S.J. Siegel, J.Q. Trojanowski, R.E. Gur, D.J. Blake, S.E. Arnold, Dysbindin-1 is reduced in intrinsic, glutamatergic terminals of the hippocampal formation in schizophrenia, J. Clin. Invest. 113 (2004) 1353–1363.
[42] M. Laruelle, W.G. Frankle, R. Narendran, L.S. Kegeles, A. Abi-Dargham, Mechanism of action of antipsychotic drugs: from dopamine D(2) receptor antagonism to glutamate NMDA facilitation, Clin. Ther. 27 (2005) S16–S24.

International Journal of Neuropsychopharmacology (2005), 8, 1–6. Copyright © 2005 CINP
doi:10.1017/S1461145705005523

BRIEF REPORT

A possible association between the −116C/G single nucleotide polymorphism of the *XBP1* gene and lithium prophylaxis in bipolar disorder

Takuya Masui[1], Ryota Hashimoto[2], Ichiro Kusumi[1], Katsuji Suzuki[1], Teruaki Tanaka[1], Shin Nakagawa[1], Hiroshi Kunugi[2] and Tsukasa Koyama[1]

[1] *Department of Psychiatry, Hokkaido University Graduate School of Medicine, Sapporo, Japan*
[2] *Department of Mental Disorder Research, National Institute of Neuroscience, National Center of Neurology and Psychiatry, Kodaira, Tokyo, Japan*

Abstract

Bipolar disorder (BPD) is a severe, chronic, and life-threatening illness, and its pathogenesis remains unclear. Recently, a functional polymorphism (−116C/G) of the X-box binding protein 1 (*XBP1*) gene was reported to be a genetic risk factor for BPD. Moreover, the endoplasmic reticulum stress responses were impaired in cultured lymphocytes from BPD patients with the −116G allele and only valproate rescued such impairment among three major mood stabilizers. In this context, we hypothesized that BPD patients with different genotypes respond differently to mood stabilizers. We investigated the association between the −116C/G polymorphism of the *XBP1* gene and lithium response in Japanese patients with BPD. We found that lithium treatment is more effective among BPD patients with the −116C allele carrier than in patients homozygous for the −116G allele. The association between the −116C/G polymorphism and clinical efficacy of mood stabilizers should be further investigated in a prospective study with a larger sample.

Received 13 October 2004; Reviewed 28 December 2004; Revised 7 February 2005; Accepted 20 February 2005

Key words: Bipolar disorder, lithium, SNP (single nucleotide polymorphism), *XBP1*.

Introduction

Bipolar disorder (BPD) is a severe, chronic, and life-threatening illness characterized by recurrent episodes of mania and depression. Despite extensive research, its pathogenesis is still unclear. Lithium is listed as a first-line agent for the treatment of BPD by American Psychiatric Association guidelines (APA, 2002). However, a significant percentage of patients with BPD show partial or no response to lithium treatment (Abou-Saleh, 1987). Psychopathological and biological markers that predict lithium response in BPD are not yet elucidated. Therefore, many researchers explored psychopathological and biological markers for lithium response in BPD, and several genetic markers are considered to be good candidates for lithium response (for reviews, see Gelenberg and Pies, 2003; Ikeda and Kato, 2003).

Recently, a functional polymorphism (−116C/G) of the X-box binding protein 1 (*XBP1*) gene that plays a pivotal role in endoplasmic reticulum (ER) stress response was shown to confer susceptibility to BPD (Kakiuchi et al., 2003). The single nucleotide polymorphism (SNP) in the promoter region of the *XBP1* gene was significantly more common in Japanese patients with BPD [odds ratio (OR) 4.6] and over-transmitted to affected offspring in trio samples of the NIMH Bipolar Disorder Genetic Initiative. The *XBP1*-dependent transcription activity of the −116G allele was lower than that of the −116C allele, and induction of *XBP1* expression after ER stress was markedly reduced in the cell with the G allele. Moreover, valproate rescued the impaired response of the cell with the G allele by inducing *ATF6*, the gene upstream of *XBP1*, although lithium and carbamazepine did not. Based on the observations, we hypothesized that BPD

Address for correspondence: R. Hashimoto, M.D., Ph.D., Department of Mental Disorder Research, National Institute of Neuroscience, National Center of Neurology and Psychiatry, 4-1-1, Ogawahigashicho, Kodaira, Tokyo, 187-8502, Japan.
Tel.: +81-42-341-2712 (ext. 5831) *Fax*: +81-42-346-1744
E-mail: rhashimo@ncnp.go.jp

patients with different genotypes respond differently to treatment with mood stabilizers such as lithium and valproate.

The aim of the study was to examine the possible association between lithium response and the XBP1 −116C/G polymorphism in patients with BPD.

Methods

Subjects

A total of 66 patients with BPD (20 BP I disorders and 46 BP II disorders) were recruited at Hokkaido University Hospital. They were composed of 38 males and 28 females with a mean age of 50.6 yr (S.D. = 11.9 yr) and a mean age at onset of 34.4 yr (S.D. = 11.4 yr). All subjects were biologically unrelated Japanese. Consensus diagnosis was made for each patient by at least two psychiatrists according to DSM-IV criteria (APA, 1994). The presence of concomitant diagnoses of mental retardation, drug dependence, or other Axis I disorder, together with somatic or neurological illnesses that impaired psychiatric evaluation, represented exclusion criteria. Patients had been treated with lithium carbonate and its serum concentration was maintained between 0.4–1.2 mequiv/l at least for 1 yr. Treatment response to lithium was determined for each patient from all available information including clinical interview and medical records, by at least two psychiatrists according to criteria described by Kato et al. (2000). Briefly, lithium responders were defined as those patients who had less frequent and/or severe relapse, including no relapse, during lithium treatment than prior to lithium treatment. Among 66 patients, 43 patients were determined as responders and 23 patients as non-responders. In the 23 non-responders, 15 patients had been treated with valproate at least for 1 yr. We secondarily evaluated the treatment response to valproate using the same criteria as for response to lithium. After complete description of the study, written informed consent was obtained from every subject. The study protocol was approved by the ethics committees of Hokkaido University Graduate School of Medicine and the National Center of Neurology and Psychiatry.

Genotyping

Venous blood was drawn from the subjects and genomic DNA was extracted from whole blood according to the standard procedures. Genotypes for the −116C/G SNP were determined using the TaqMan 5′-exonuclease allelic discrimination assay, described previously (Hashimoto et al., 2004). Briefly, probes and primers for detection of the polymorphism were: forward primer 5′-CTGTCACTCCGGATGGAAATA-AGTC-3′, reverse primer 5′-ATCCCTGGCCAAAGG-TACTTG-3′, probe 1 5′-VIC-CTCCCGCACGTAAC-MGB-3′, and probe 2 5′-FAM-TCCCGCAGGTAAC-MGB-3′. PCR cycling conditions were: 95 °C for 10 min, 45 cycles of 92 °C for 15 s and 60 °C for 1 min.

Statistical analysis

Difference in clinical features between responders and non-responders to lithium treatment was analysed using the χ^2 tests for categorical variables and the t tests for continuous variables. The presence of Hardy–Weinberg equilibrium was examined by using the χ^2 test for goodness of fit. Genotype and allele distributions between responders and non-responders to lithium treatment were analysed by the χ^2 test for independence. Association between genotype and serum lithium levels was analysed by analysis of variance (ANOVA). All p values reported are two-tailed. Statistical significance was defined at $p<0.05$.

Results

The clinical characteristics of patients with BPD are shown in Table 1. Significant differences were not found in clinical features between patients who were defined as responders and non-responders to lithium treatment. Allele frequencies and genotype distributions of the −116C/G polymorphism of the *XBP1* gene among responders and non-responders to lithium treatment are shown in Table 2. The genotype distributions for the total patients, responders, and non-responders were both in Hardy–Weinberg equilibrium (total patients: $\chi^2=1.19$, d.f. = 1, $p=0.28$; responders: $\chi^2=1.8$, d.f. = 1, $p=0.18$; non-responders: $\chi^2=0.13$, d.f. = 1, $p=0.72$). Serum lithium levels in responders did not differ among *XBP1* genotypes [C/C 0.64 (S.D. = 0.10) mequiv/l; C/G 0.66 (S.D. = 0.24) mequiv/l; G/G 0.53 (S.D. = 0.18) mequiv/l; $F=1.83$, $p=0.17$, ANOVA]. On the other hand, there was a trend towards increased serum lithium levels in non-responders homozygous for the −116G allele [C/C 0.48 mequiv/l ($n=1$); C/G 0.53 (S.D. = 0.16) mequiv/l; G/G 0.69 (S.D. = 0.19) mequiv/l], but it did not reach statistical significance ($t=2.0$, d.f. = 20, $p=0.059$, t test comparing patients with C/G and G/G).

There was a trend towards an increased frequency of the −116C allele in the responders rather than non-responders ($\chi^2=3.72$, d.f. = 1, $p=0.054$; OR 2.18, 95% CI 0.98–4.87). Subsequent Mantel–Haenszel tests showed a differential genotype distributions between

Table 1. Background and clinical characteristics of bipolar (BP) patients

	Lithium-treated patient			Responders vs. non-responders
	Total (66)	Responder (43)	Non-responder (23)	
Sex				
Males	38 (57.6%)	28 (65.1%)	10 (43.5%)	$\chi^2=2.87$, d.f.=1, $p=0.09$
Females	28 (42.4%)	15 (34.9%)	13 (56.5%)	
Diagnosis				
BP I	20 (30.3%)	14 (32.6%)	6 (26.1%)	$\chi^2=0.30$, d.f.=1, $p=0.59$
BP II	46 (69.7%)	29 (67.4%)	17 (73.9%)	
Psychotic features				
Present	7 (10.6%)	6 (14.6%)	1 (4.3%)	$\chi^2=1.46$, d.f.=1, $p=0.23$
Absent	59 (89.4%)	37 (85.4%)	22 (95.7%)	
History of rapid cycling				
Present	10 (15.2%)	4 (9.3%)	6 (26.1%)	$\chi^2=3.28$, d.f.=1, $p=0.07$
Absent	56 (84.8%)	39 (90.7%)	17 (73.9%)	
Medication				
Lithium monotherapy	14 (21.2%)	11 (25.6%)	3 (13.0%)	$\chi^2=1.41$, d.f.=1, $p=0.24$
Presence of co-administration[a]	52 (78.8%)	32 (74.4%)	20 (87.0%)	
				t test
Age (yr)[b]	50.6±11.9	51.1±11.3	49.7±13.1	$t=0.44$, d.f.=64, $p=0.66$
Age at onset (yr)[b]	34.4±11.4	34.0±11.7	35.1±11.0	$t=0.38$, d.f.=64, $p=0.70$
Serum lithium concentration[b] (mequiv/l)	0.62±0.20	0.62±0.21	0.62±0.19	$t=0.03$ d.f.=64, $p=0.98$

[a] Aditional administration of valproate, carbamazepine, antidepressants, antipsychotics are included.
[b] Continuous variables are shown as mean±S.D.

responders and non-responders ($\chi^2=4.30$, d.f.=1, $p=0.038$). Thus, we examined the C allele carriers and non-carriers separately, and found that the C allele carriers were significantly more common in the responder group than the non-carriers ($\chi^2=4.34$, d.f.=1, $p=0.037$; OR 3.00, 95% CI 1.05–8.58).

The genotype distributions among responders and non-responders to valproate treatment are shown in Table 3. There was no association between the −116C/G polymorphism of the *XBP1* gene and response to valproate ($\chi^2=1.25$, d.f.=2, $p=0.54$).

Discussion

We investigated the possible association between the *XBP1* gene and the response to lithium treatment in BPD for the first time. Our results suggest that lithium treatment is more effective in BPD patients with the −116C allele of the *XBP1* gene than in patients homozygous for the G allele.

Kakiuchi et al. (2003) proposed that impaired response against ER stress in BPD patients with the G allele might be one of the possible cellular and molecular pathophysiology of BPD. Among three representative mood stabilizers, only valproate rescued this impairment of ER stress response in cultured lymphocytes, although lithium or carbamazepine did not. These findings suggested that the effectiveness of lithium on BPD patients with the G allele might be weaker than those with the C allele. Our clinical observations were consistent with the proposed mechanisms. A possible explanation for the mechanisms of the better efficacy of lithium treatment in −116C carriers is that −116C carrier patients might have other cellular and molecular impairments, which lithium could influence in the nervous system, e.g. inhibition of glycogen synthase kinase-3, inositol monophosphatase and *N*-methyl-D-aspartate receptor activity, activation of the BDNF/Trk pathway, or enhancement of neurogenesis and neuronal progenitor